

Structural, optical and electrical study of nanocrystalline SnSe thin films: effect of pH

DEEP SHIKHA^{a,b*}, J. K. SHARMA^a, J. SHARMA^c

^aDepartment of Physics, Maharishi Markandeshwar University, Mullana, Ambala-133207, India

^bPG Department of Physics, Sri Guru Teg Bahadur Khalsa College, Anandpur Sahib-140118, India

^cDepartment of Nanotechnology, Sri Guru Granth Sahib University, Fatehgarh Sahib – 140407, India

Abstract. Nanocrystalline tin selenide (SnSe) thin film form has been synthesized by chemical bath deposition technique. The thin film is deposited on glass substrates in an aqueous alkaline medium using sodium selenosulphate as Se^{2-} ion source. The comparison of structural, optical and electrical properties of SnSe thin films at different pH of the solution has been studied. Structural and morphological characterization is done by X-ray diffraction (XRD). The films were polycrystalline with peaks corresponding to the orthorhombic phase. The grain size increases with increase of pH. The microstructural parameters like strain and dislocation density were also calculated and compared at different pH. The optical band gap of nanocrystalline SnSe thin films at different pH has been measured using UV – VIS absorbance spectroscopy and steady state and transient photoconductivity has been discussed in electrical properties.

(Received January 11, 2015; accepted February 10, 2016)

Keywords: Structural, Optical, Electrical, Chemical bath deposition, Tin selenide

1. Introduction

$\text{A}^{\text{II}}\text{B}^{\text{VI}}$ semiconductors were widely investigated, as potential candidates for optoelectronic applications [1], particularly for photovoltaic cells [2]. The material in this class, especially tin selenide (SnSe) has been studied in the form of both single crystal [3] and thin films [3-5]. Tin selenide (SnSe) has been used as memory switching devices, infrared electronic devices, light emitting devices (LED) and holographic recording systems [6-9]. It could also be used in photo-electrochemical cells, decreasing the photo corrosion reaction [7]. Tin selenide exists as a layered compound with an orthorhombic crystal structure. Different methods of preparation have been described in the literature: chemical bath deposition [4], atomic layer deposition [8], thermal evaporation [10-11], vacuum evaporation [12] and solvothermal routes [3]. Chemical bath deposition is the cheapest known technique for preparation of powder and thin films. It is a slow process, which facilitates a better orientation of the crystallites with an improved grain structure. Depending on the deposition condition, the film growth can take place by ion-ion condensation or by adsorption of colloidal particles (cluster by cluster) from the solution onto substrates. Many of these films proved to be of comparable quality with those produced by other sophisticated and expensive methods. Present paper give comparison of morphological, optical and electrical study of the tin selenide thin films obtained at different pH of the solution by a simple chemical route.

2. Experimental detail

Tin selenide thin films were deposited onto cleaned, spectroscopic grade glass substrates. All chemicals used were of AR grade. To synthesize nanocrystalline SnSe we have employed the chemical bath deposition (CBD) technique using tin chloride and sodium selenosulphate as precursors of Sn^{2+} and Se^{2-} ions in the reaction system. To prepare sodium selenosulphate solution, 15 g of sodium sulfite in 200 ml water was refluxed with 5 g of selenium for almost 10 hours at 75°C . The mixture remained under constant stirring throughout the reflux process. Selenosulphate is produced according to the following reaction:



Unreacted selenium is filtered off and selenosulphate solution is placed in air tight bottle. It is recommended to make small volumes of selenosulphate stock solution to be used within 3–4 days. To deposit SnSe at different pH, sodium hydroxide (1M) solution in deionized water is prepared. This solution is used to maintain alkaline media of pH at three different values 11.0, 11.4 and 11.8. In three different beakers, sodium hydroxide is added drop wise to 0.94g of tin chloride dissolved in 10 ml water to obtain an alkaline media of pH 11.0, 11.4 and 11.8. Then 10 ml of sodium selenosulphate solution is introduced into these three different beakers and glass substrates are mounted vertically in these beakers. The film growth was carried out in all the beakers at temperatures 45°C . A dark brown precipitate gradually fills the baths and turns black after 20

min. During deposition period the beakers was kept undisturbed for a time period of 2.5 hours. The as-deposited SnSe films are specularly reflective and black in appearance when observed under white light. The deposited films were tested for adhesion by subjecting it to a steady stream of distilled water. Diffraction patterns of intensity versus 2θ were recorded with a XPERT-PRO diffraction, using a monochromatic X-ray beam having Cu $K\alpha_1$ radiation with $\lambda = 1.54060 \text{ \AA}$ (40 mA, 45 kV). A continuous scan mode was used to collect 2θ data from 20° to 80° . The microstructure of the samples were studied by using a scanning electron microscope (JSM 6610LV) operating at 15KV. The absorption spectra were recorded using double beam spectrophotometer [SPECORD-250] in the transmission range 200-800 nm for both samples. The electrical measurements of these thin films are carried out in a specially designed metallic sample holder where heat filtered white light of intensity 8450 lx (200W tungsten lamp) is shone through a transparent glass window. A vacuum of about 10 mbar was maintained throughout these measurements. Light intensity was measured using a digital luxmeter. Planar geometry of the films (length ~ 0.74 cm; electrode gap ~ 1 mm) is used for the electrical measurements. Al electrodes are used for the electrical contacts because Al metal does not diffuse inside the material. These contacts are made by diffusion technique. The dark- and photocurrent was noted using a digital picoammeter

3. Result and discussion

3.1 Structural study

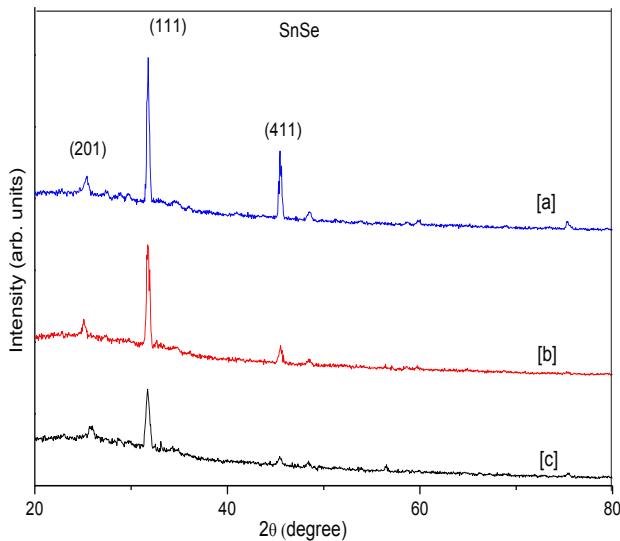


Fig. 1. XRD pattern of SnSe thin films deposited at [a] pH = 11.0, [b] pH = 11.4 and [c] pH = 11.8.

Fig. 1 represents the diffraction pattern of SnSe thin films forms deposited at different pH values (11.0, 11.4 and 11.8) of the bath. The observed d values of thin films

form at different values of pH are in good agreement with the standard values for the orthorhombic structure of SnSe [4, 6, 9]. The Structural parameters of SnSe thin films deposited at different pH have been listed in table 1. Comparing the d -values with standard values indicates that [111] is the preferred orientation in these samples. The diffusion background and broad peak appearing at low angles are due to the amorphous glass substrate.

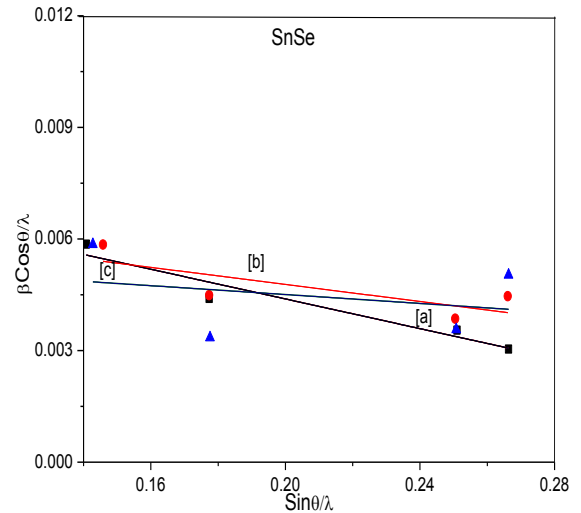


Fig. 2. Plots between $(\beta \cos \theta) / \lambda$ and $(\sin \theta) / \lambda$ for SnSe thin films deposited at [a] pH = 11.0, [b] pH = 11.4 and [c] pH = 11.8.

Information about strain and particle size are obtained from the full width at half maximum (FWHM) of the diffraction peaks. The FWHM (β) can be expressed as a linear combination of the contributions from the strain (ϵ) and particle size (L) as in relation [13]:

$$\frac{\beta \cos \theta}{\lambda} = \frac{1}{L} + \frac{\epsilon \sin \theta}{\lambda} \quad (2)$$

The reciprocal of intercept on the $(\beta \cos \theta) / \lambda$ axis gives the average particle size. Fig. 2 represents the plots of $(\beta \cos \theta) / \lambda$ vs. $(\sin \theta) / \lambda$ for SnSe thin films at different pH values (11.0, 11.4 and 11.8) which are straight lines. The slope of these plots give the amount of residual strain, Stress and strain are almost always present in all thin films deposited at different pH. In the majority of cases, these stresses are residual stresses introduced into the system during deposition or subsequent processing. In our case the particle size and strain calculated from fig. 2 are listed in table 1. The crystallite size increases with increase of pH values from 11 to 11.8 which shows the improvement in crystallinity. At higher pH (in alkaline solution), generally selenosulphate decomposition is faster [14]. It results in faster rate of reaction and increases particle size. The negative value of residual strain for the films deposited at different pH indicates the compressive strain. If the film deposited is free from impurities, the compressive strain is generated at the thin film substrate interface, when the very small crystallites are bonded to substrate, due to

surface tension. The strain decreases with increase in pH of the solution (shown in table 1).

The dislocation density δ defined as the length of dislocation lines per unit volume of the crystal can be evaluated from the particle size D by the relation [15]:

$$\delta = 1/D^2 \quad (3)$$

The minimum value of dislocation density are observed for the films with the highest pH value as shown in Table 1 which means the degree of imperfection is minimum in the films with highest pH value (pH = 11.8).

The lattice parameter a , b and c is determined for the orthorhombic structure by using the following expression:

$$\frac{1}{d^2} = \frac{h^2}{a^2} + \frac{k^2}{b^2} + \frac{l^2}{c^2} \quad (4)$$

Table 1. Various structural and optical parameters of SnSe thin films deposited at different pH of the solution.

pH	D (nm)	Strain ($\text{lin}^{-2} \text{m}^{-4}$)	δ (lines/ m3)	Lattice Parameters			E_g (eV)
				a(\AA)	b(\AA)	c(\AA)	
11.0	11.38	-1.99×10^{-2}	7.72×10^{15}	10.90	4.58	3.78	2.25
11.4	14.14	-1.14×10^{-2}	5.00×10^{15}	10.95	4.64	3.71	2.04
11.8	17.54	-5.90×10^{-3}	3.25×10^{15}	10.95	4.42	3.90	1.82

where h , k , and l are the Miller indices of the lattice plane.

The lattice spacing (d) is calculated from the Bragg's formula [16]:

$$d = \frac{\lambda}{2 \sin \theta} \quad (5)$$

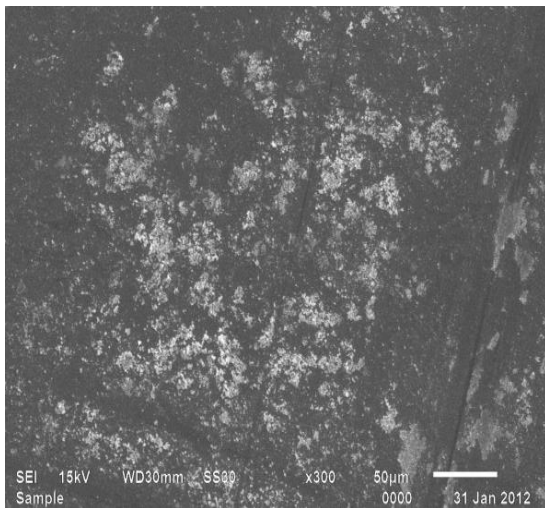


Fig. 3. SEM micrograph of SnSe thin film at pH = 11.4.

The SEM micrograph of film at pH = 11.4 have been taken which shows a distribution of particles covers the surface of the substrate completely. No pin holes or cracks could be observed in the film.

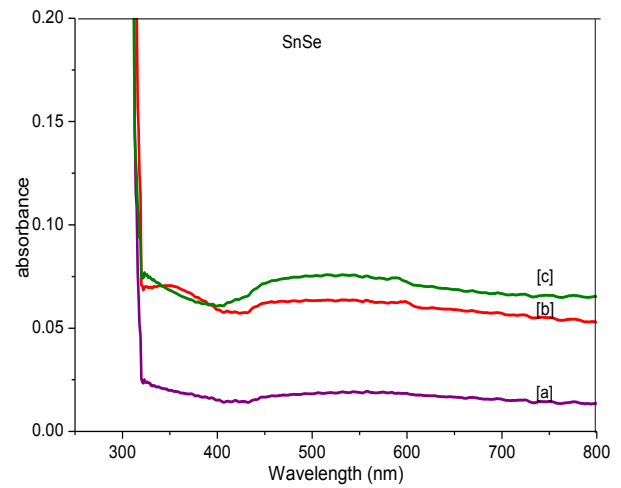


Fig. 4. Absorbance spectra of SnSe thin films at [a] pH= 11.0 [b] pH = 11.4 and [c] pH = 11.8.

3.2 Optical study

Fig. 4 represents the absorption spectra of SnSe thin films at different pH. From the absorption data, nearly at the fundamental absorption edge, the values of absorption coefficient (α), are calculated in the region of strong absorption using the relation:

$$\alpha = 2.303 \frac{A}{d} \quad (6)$$

The fundamental absorption, which corresponds to the transition from valence band to conduction band, can be used to determine the band gap of the material.

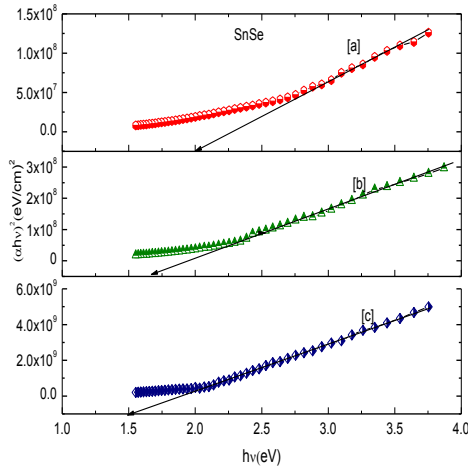


Fig.5. The plots of $(\alpha hv)^2$ vs. hv for SnSe thin films at [a] pH= 11.0 [b] pH =11.4 and [c] pH = 11.8.

The relation between α and the incident photon energy (hv) can be written as [17]:

$$\alpha = \frac{A(h\nu - E_g)^n}{h\nu} \quad (7)$$

where A is a constant, E_g is the band gap of the material and the exponent n depends on the type of transition.

The n may have values 1/2, 2, 3/2 and 3 corresponding to the allowed direct, allowed indirect, forbidden direct and forbidden indirect transitions, respectively. The value of band gap E_g is calculated by extrapolating the straight line portion of $(\alpha hv)^{1/n}$ vs. hv graph to hv axis taking $n = 1/2$ (0.5). Fig. 5 show the plots of $(\alpha hv)^2$ vs. hv for SnSe films deposited at three different pH. The value of E_g at different pH is inserted in Table 1. Clearly, the observed values of E_g are higher than the value of bulk optical gap of SnSe (1.68 eV)[18] due to quantum confinement in the SnSe nanocrystallites. The optical band gap decreases from 2.0 eV to 1.5 eV with the increase in pH of the solution as given in table 1. and blue shift in the fundamental edge has been observed. The optical band gap decreases because the particle size increases with increase of pH of the solution.

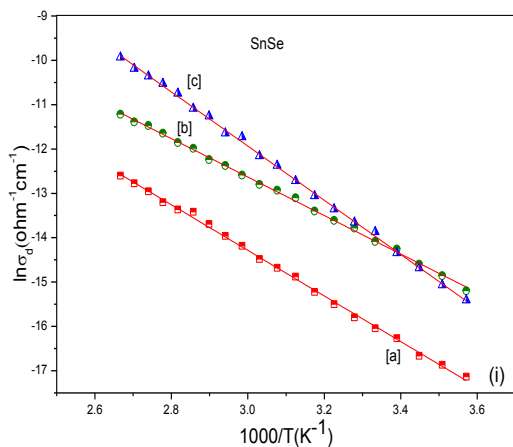


Fig. 6. Plot of $\log \sigma_d$ vs. $(1000/T)$ of SnSe films deposited at [a] pH = 11.0 [b] pH =11.4 and [c] pH =11.8.

3.3 Electrical properties

3.3.1 Steady state photoconductivity

Fig. 6 and Fig. 7 shows the temperature dependence of dark conductivity (σ_d) and photo conductivity (σ_{ph}) for SnSe thin films at different pH. The electrical conductivity shows typical Arrhenius type of activation

$$\sigma_d = \sigma_0 \exp\left(-\frac{\Delta E}{kT}\right) \quad (8)$$

where ΔE is the activation energy for conduction and k is the Boltzmann's constant. Fig. 6 and Fig. 7 shows the variation of σ_d and σ_{ph} against $1000/T$ for SnSe thin films deposited at different pH. The plots of $\ln \sigma_d$ vs. $1000/T$ and $\ln \sigma_{ph}$ vs. $1000/T$ are straight lines in the measured temperature range. This implies that the conduction in SnSe thin films is an activated process having single activation energy. The activation energies (ΔE_d and ΔE_{ph}) for dc conduction have been calculated from the slopes of $\ln \sigma_d$ vs $1000/T$ and $\ln \sigma_{ph}$ vs. $1000/T$ curves. The values of σ_d , σ_{ph} , ΔE_d and ΔE_{ph} are listed in Table 2. The values of σ_d and σ_{ph} at room temperature increases as the pH of SnSe thin films increases from 11.0 to 11.8. The increase in conductivity with the increase in pH of Sn^{2+} ion is due to the increase in particle size of SnSe nanocrystals. The effect of size on electrical conductivity of nanostructures is based on the following mechanisms: surface scattering, quantized conduction, Coulomb charging and tunneling, widening and discrete band gap and change of microstructure.

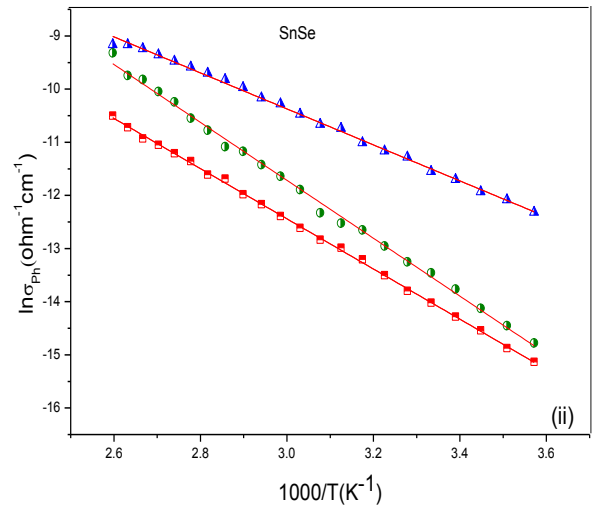


Fig. 7. Plot of $\log \sigma_{ph}$ vs. $(1000/T)$ of SnSe films deposited at [a] pH = 11.0 [b] pH =11.4 and [c] pH =11.8.

It is also clear from Table 2 that there is increase in the value of activation energy (ΔE) with the increase in the pH. The similar type of results has been reported by some workers [19].

3.3.2 Transient photoconductivity

Fig. 8 shows the rise and decay curves of I_{ph} for SnSe thin films at different pH of the solution. I_{ph} rises to a steady state value and a peak is observed in rise curves of SnSe films deposited at different pH of the solution. During decay, the photocurrent does not reach zero for a long time after the incident light is switched off. A persistent photocurrent is observed in all the cases. This type of photoconductive decay has also been reported in various other semiconductors [20-21]. In the present case, the non-exponential decay of photoconductivity is observed.

The values of τ_d at different times have been calculated using equation

$$\tau_d = - \left[\frac{1}{I_{ph}} \frac{dI_{ph}}{dt} \right]^{-1} \quad (9)$$

for SnSe thin films deposited at different pH of the solution from the slopes (at different times) of decay curves of Fig.8. The decay times observed for n-SnSe thin films, deposited at different pH, are found to be time dependent. The value of τ_d increases with time, which confirms the non-exponential decay of photocurrent. Fig. 9 shows the plots of $\ln \tau_d$ vs. $\ln t$ for all samples at intensity 8450 Lux. The extrapolation of the curves at $t = 0$, give the values of the decay life time [22] and are found to be

1.88, 2.59 and 2.72 seconds for films deposited at pH of the solution 11.0, 11.4 and 11.8. Clearly, the carrier life time increases with increasing pH of the solution (size).

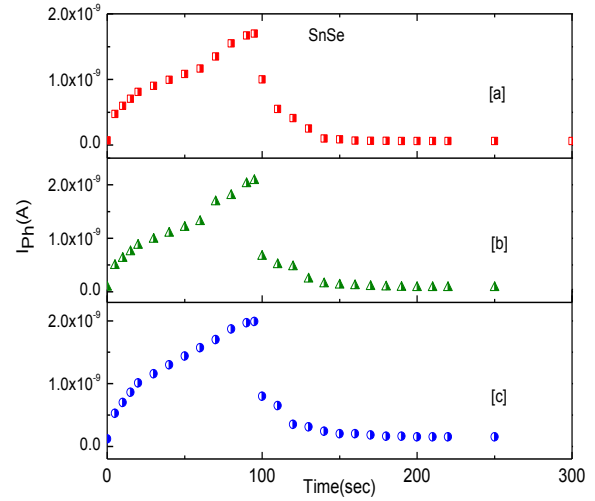


Fig. 8. The rise and decay curves of I_{ph} for SnSe thin films at [a] pH = 11.0, [b] pH = 11.4 and [c] pH = 11.8.

The straight lines in Fig. 9, obey a power law of the form t^{-N} , with $N = d(\ln \tau_d / \ln t)$ and the values of N are found to be 0.565, 0.342 and 0.447 at pH of the solution 11.0, 11.4 and 11.8 respectively.

Table 2. Variation of various electrical parameters for SnSe thin films deposited at different pH values of the solution.

pH	σ_d ($\Omega^{-1}cm^{-1}$)	ΔE_d (eV)	σ_{ph} ($\Omega^{-1}cm^{-1}$)	ΔE_{ph} (eV)	σ_{ph} / σ_d	$\ln \tau_{d(t=0)}$ (sec)
11.0	2.05×10^{-6}	1.02	4.87×10^{-6}	0.93	2.37	1.88
11.4	6.32×10^{-6}	0.86	1.92×10^{-5}	1.08	3.04	2.59
11.8	1.81×10^{-5}	1.21	4.38×10^{-5}	0.67	2.43	2.72

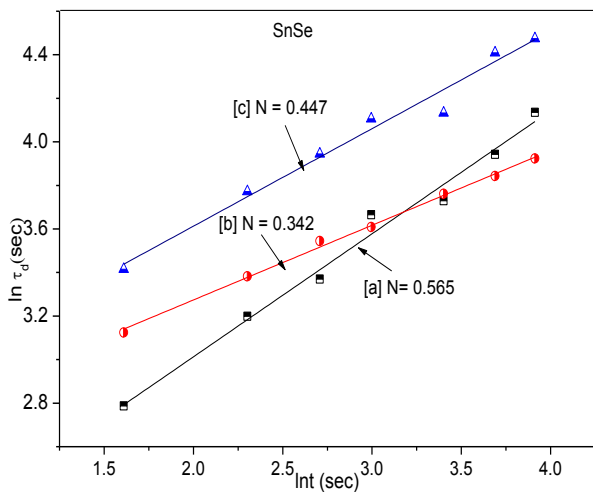


Fig. 9. Plot of τ_d vs. $\ln t$ for SnSe thin films deposited at different pH [a] 11.0, [b] 11.4 and [c] 11.8.

4. Conclusions

Comparison of observed d -values with the standard values confirms orthorhombic structure of SnSe with [111] as preferred orientation in these samples. The average crystallite size for these samples has been calculated and increases from 11.38 nm to 17.54 nm with increase of the pH value of the solution from 11.0 to 11.8. The microstructural parameters i.e dislocation density and strain decreases with increase of particle size (or increase of pH) which means that the degree of imperfection is minimum in the films with highest pH value. The band gap decreases from 2.25 eV to 1.82 eV with the increase in pH and blue shift in the fundamental edge has been observed. For steady state conductivity, the values of dark conductivity (σ_d) and photoconductivity (σ_{ph}) at different pH are calculated and increases with increase of pH of the solution. In transient conductivity, in the rise and decay curves, the value of decay life time τ_d increases with time,

which confirms the non-exponential decay of photocurrent and the carrier life time increases with increasing pH of the solution.

Acknowledgements

The author acknowledges the support provided by Mr. S.C. Sood of Ambala College of Engineering, Mithapur for the completion of this work.

References

- [1] N. Babentsov, *Quantum Electronics & Optoelectronics*, **3**, 94(2006).
- [2] S. Antohe, S. Iftimie, V. Ghenescu, R. Constantineanu, M. Gugiu, M. Ion, I. Stan, A. Radu, L. Ion, *Romanian Reports in Physics* **64**, Supplement, 1153(2012).
- [3] W. Wang, Y. Geng, Y. Qian, C. Wang, X. Liu, *Mater. Res. Bull.*, **34**, 403(1999).
- [4] D. Shikha, R. P. Chauhan, Jeewan Sharma, *Optoelectron. Adv. Mater. – Rapid Comm.*, **6**(7-8), 734(2012).
- [5] B. Subramanian, T. Mahalingam, C. Sanjeeviraja, M. Jayachandran, M. J. Chockalingam, *Thin Solid Films* **357**, 119(1999).
- [6] Z. Zainal, S. Nagalingam, A. Kassim, M. Z. Hussein, W. M. M. Yunus, *Solar Energy Mater. Solar Cells*, **81**, 261(2004).
- [7] K. Zweibel, *Solar Energy Mater. Solar Cells*, **63**, 375 (2000).
- [8] T. Lindgren, M. Larsson, S. Lindquist, *Solar Energy Mater. Solar Cells* **73**, 377(2002).
- [9] N. R. Mathews, *Solar Energy.*, **86**, 1010(2011).
- [10] D.P.Padiyan, A.Marikani, K.R.Murali, *Cryst.Res.Technol*, **35**(8), 949(2000).
- [11] N. Kumar, V. Sharma, U. Parihar, R. Sachdeva, N. Padha and C. J. Panchal, *J. Nano-Electron.*, **3**(1), 110 (2011).
- [12] S. K. Tripathi, S. K. Tripathi. Thakur, G. Singh, J. Sharma, V. Sharma, K. P. Singh, *J. Optoelectron. Adv. Mater.*, **7**(4), 2095(2005).
- [13] G. S. S. Saini, N. Goya, *J. Cryst. Growth*. **306**, 68(2007).
- [14] Jeewan Sharma, G. S. S. Saini, N. Goyal, S. K. Tripathi, *J. Optoelectron. Adv. Materials*, **9** (10), 3194(2007).
- [15] Charita Mehta, *Thin Films for Solar Cell Applications* **123** (2009).
- [16] S.B. Quadri, E.F. Skelton, D. Hsu, A.D. Dinsmore, J. Yang, H.F. Gray, B.R. Ratna, *Phys.Rev. B***60**, **9191** (1999).
- [17] Nicolae Tigau. *Romanian Journal of Physics*, **53**(1), 209 (2008),
- [18] K. Ananthi, S. Dhanapandian, C. Manoharan, K. Thilagavathy, N. Muthukumarasamy, K.R. Murali, *International Journal of Current Physical Sciences*, **2**(3), 14 (2012).
- [19] J. Sharma, G. Singh, A. Thakur, G. S. S. Saini, N. Goyal, S. K. Tripathi, *J. Optoelectron. Adv. Mater.* **7**(4), 2085 (2005).
- [20] Nicolae Tigau, *Romanian Journal of Physics*, **53**(1), 203 (2008).
- [21] M. Igalson, *Solid State Communications* **44**, 247 (1982).
- [22] A. Ganjoo, K. Shimakawa, K. Kitano and E.A. Davis, *J. Non-Cryst. Solids* **299**, 917 (2002).
- [23] A. Rose, *Interscience*, New York, 1963.

Corresponding author: deep_shikha79@yahoo.co.in